Polymer 49 (2008) 3762–3769

Contents lists available at ScienceDirect

Polymer

journal homepage: www.elsevier.com/locate/polymer

Effect of organoclay purity and degradation on nanocomposite performance, Part 2: Morphology and properties of nanocomposites

Lili Cui [a], D.L. Hunter [b], P.J. Yoon [b], D.R. Paul [a,*]

[a] Department of Chemical Engineering, Texas Materials Institute, The University of Texas at Austin, Austin, TX 78712, United States
[b] Southern Clay Products, 1212 Church Street, Gonzales, TX 78629, United States

ARTICLE INFO

Article history:
Received 31 March 2008
Received in revised form 10 June 2008
Accepted 18 June 2008
Available online 24 June 2008

Keywords:
Nanocomposites
Organoclay degradation
Purification

ABSTRACT

Part 1 of this series showed that the purification level and surfactant loadings of organoclays significantly affect their thermal stability; the higher rate of degradation of as-received commercial organoclay is primarily a result of excess surfactant that is intentionally or unintentionally part of the commercial organoclay. Polypropylene nanocomposites and nylon 6 nanocomposites were formed through melt processing to assess the practical consequences, in terms of nanocomposite formation and performance, of using a purified version of the organoclay with no excess surfactant and a lower rate of thermal degradation versus using the as-received organoclay. The properties and morphology of polymer–clay nanocomposites based on both as-received and purified organoclays were evaluated by TEM, WAXS, and mechanical testing. The results from the different techniques were generally consistent with each other suggesting that the differences in thermal stability of organoclays do not appear to have a significant effect on the morphology and properties of the nanocomposites formed from them.

© 2008 Elsevier Ltd. All rights reserved.

1. Introduction

Part 1 of this series dealt with the rate of thermal degradation of surfactants used to form commercial organoclays using thermogravimetric analysis. Previous reports showed evidence that purification of organoclays improves their thermal stability [1–3]; to a certain extent, the results of Part 1 support this conclusion [4]. This work showed that the higher rate of degradation of as-received commercial organoclay is primarily a result of excess surfactant that is intentionally or unintentionally part of the commercial organoclay. The purpose of this paper is to assess the practical consequences, in terms of nanocomposite formation and performance, of using a purified version of the organoclay with no excess surfactant and a lower rate of thermal degradation versus using the as-received organoclay. Purification of organoclays by simple methanol washing was shown to be nearly as effective for removing the excess surfactant as a more rigorous and time consuming Soxhlet extraction process [4]. Such purification procedures significantly change the thermal stability of the as-received organoclay. Whether this excess surfactant and the associated higher degradation rate have significant impact on the morphology and properties of nanocomposites formed from them is explored here. Nanocomposites based on as-received organoclays and purified organoclays are compared. Previous studies in our laboratory showed that nylon 6-based nanocomposites have the best exfoliation when formed from an organoclay based on a surfactant with only one long alkyl tail [5,6]; on the other hand, polyolefin matrices give better exfoliation with organoclays based on a surfactant with two or more long alkyl tails [7–10]. A series of organoclays based on a surfactant with two hydrogenated tallow tails in varying levels of excess were selected to form polypropylene nanocomposites. Likewise, a series of organoclays based on a single tail, either hydrogenated tallow or a 16-carbon alkyl, were similarly used to form nylon 6 nanocomposites. The properties and morphology of polymer–clay nanocomposites based on both as-received and purified organoclays were evaluated by various techniques and compared.

2. Experimental

2.1. Materials

A brief description of the polymers used in this study is given in Table 1. In one series, a commercial injection molding grade of polypropylene supplied by Basell served as the matrix, while a PP-*g*-MA containing 1 wt% maleic anhydride groups supplied by Crompton is used as the compatibilizer for promoting exfoliation of the organoclay. In a second series, a commercial high molecular weight grade of nylon 6 from Honeywell was selected to form nanocomposites.

* Corresponding author. Tel.: +1 512 471 5392; fax: +1 512 471 0542.
E-mail address: drp@che.utexas.edu (D.R. Paul).

0032-3861/$ – see front matter © 2008 Elsevier Ltd. All rights reserved.
doi:10.1016/j.polymer.2008.06.028

Table 1
Polymers used in this study

Materials (designation used here)	Commercial designation	Supplier	Properties
Polypropylene (PP)	Pro-Fax PH020	Basell	MI = 37 Density = 0.902 g/cm^3
Maleic anhydride grafted polypropylene (PP-*g*-MA)	PB3200	Crompton	MI = 105 Density = 0.91 g/cm^3 MA content = 1.0 wt% $\overline{M}_w$ = 90,000 MWD ≈ 2.7
Nylon 6 (PA-6)	Capron B135WP	Honeywell	MI = 1.2 $\overline{M}_n$ = 29,300

Organically modified clays, formed by an ion exchange reaction between sodium montmorillonite (Na-MMT) and ammonium surfactants, were generously donated by Southern Clay Products, Inc. Descriptions of these organoclays are given in Part 1 [4]. A similar nomenclature system as used in prior papers [5,9,11] is adopted to describe the chemical structure of the ammonium cations in a concise manner. The letter M represents methyl substituent. The letter HT denotes the tallow-based product, which is predominantly composed of chains with 18 carbons (~65%) and the majority of the double bounds have been hydrogenated; while C16 represents a 16-carbon alkyl chain. The level of surfactant contained in the organoclays is designated by the milliequivalent ratio (MER) defined as the milliequivalents of ammonium cations per 100 g of clay [4,5].

The selected as-received organoclays were purified by using a single methanol wash to remove excess surfactant. The purification method involved suspending the organoclay in methanol, with magnetic stirring at room temperature for 1 h, then setting the mixture aside until the suspension stratified followed by decanting the top clear solution. Afterwards, the white precipitate was washed with methanol and distilled water again while being filtered. The final product was dried at room temperature and then under vacuum at 80 °C overnight. The hard white cake formed was ground into a fine powder prior to be used in melt processing.

2.2. Melt processing

Polypropylene and nylon 6 nanocomposites were both prepared by melt compounding in a Haake, co-rotating, intermeshing twin screw extruder ($D = 30$ mm, $L/D = 10$) at a screw speed of 280 rpm and a feed rate of 1000 g/h, with all the components added at the same time [12–17]. All the materials were dried in a vacuum oven for a minimum of 24 h prior to the compounding.

Polypropylene nanocomposites were formed from the $M_2(HT)_2$ organoclays at a melt processing temperature of 190 °C, while nylon 6 nanocomposites were formed from the $M_3(HT)_1$ or $M_3(C16)_1$ organoclays at 240 °C. The MER levels of the organoclays were varied from a minimum value for the purified material upwards by using various as-received commercial products. Tensile (ASTM D638) and Izod (ASTM D256) specimens were formed using an Arburg Allrounder 305-210-700 injection molding machine. After molding, the specimens were immediately sealed in a polyethylene bag and placed in a vacuum desiccator for a minimum of 24 h prior to mechanical testing.

The data below are reported in terms of the weight percent montmorillonite (MMT) in the composites rather than the amount of organoclay, since the silicate is the reinforcing component.

2.3. Characterization

WAXS scans were obtained using a Scintag XDS 2000 diffractometer in reflection mode with an incident X-ray wavelength of 1.542 Å at a scan rate of 1.0°/min. X-ray analyses were performed on the skin of the major faces of the injection molded Izod bars while the organoclays were analyzed in powder form.

Tensile tests were performed on an Instron model 1137 machine upgraded for computerized data acquisition. Modulus values were determined using an extensometer at a crosshead speed of 0.51 cm/min. Elongation at break was measured at crosshead speeds of both 5.1 cm/min and 0.51 cm/min. Notched Izod impact tests were performed at room temperature with a TMI Izod tester (6.8-J hammer and 3.5 m/s impact velocity) according to ASTM D 256. As common practice, Izod bars were cut in half to generate more samples. Depending on whether a significant difference is shown between the far end and gate end of the bars, data are either shown as averages of all values or reported as separately averaged values for far-end and gate-end specimens. Data reported here represent an average from measurements on at least five specimens.

TEM images were obtained using a JEOL 2010F transmission electron microscope operating at an accelerating voltage of 120 kV. Ultra-thin sections (~50 nm) were cut from the central part of the Izod bars in the plane parallel to the flow direction under cryogenic conditions using an RMC PowerTome XL microtome.

3. Results and discussion

The thermal degradation studies from Part 1 [4] show that the organoclay stability is dramatically improved by purification; the main effect appears to be the removal of excess surfactant that is not ionically bound to the montmorillonite. The question here is whether these differences in stability or the presence of excess surfactant affects the properties and morphology of the nanocomposites formed from as-received versus purified organoclays. The following results and discussion are focused on answering this question.

3.1. Polypropylene nanocomposites

Three commercially available organoclays are included to explore the effect of purification on the morphology and properties of polypropylene nanocomposites. The three commercial organoclays, formed through the modification of sodium montmorillonite with various amounts of $M_2(HT)_2^+Cl^-$ surfactant, are designated as Cloisite 20A, 15A and 6A, which have MER values of 95 mequiv/100 g, 125 mequiv/100 g, and 140 mequiv/100 g of clay, respectively. Cloisite 20A was purified using the procedures described earlier, and the MER after purification was determined by ash analysis to be 88 mequiv/100 g of clay. Besides these commercial organoclays, an experimental organoclay modified by $M_2(HT)_2^+MeSO_4^-$ surfactant with an MER of 140 mequiv/100 g of clay is also included in some of the discussions below. Although this experimental organoclay has a high loading of surfactant, due to the methyl sulfate anions in the free surfactant of the organoclay this organoclay is considerably more thermally stable [4] than the commercial organoclay Cloisite 6A, which has the same surfactant loading but is modified by the $M_2(HT)_2^+Cl^-$ surfactant.

All the PP nanocomposites were prepared at several MMT loadings to obtain a more complete picture of the relative benefit of each organoclay. The ratio of PP-*g*-MA to clay was set at 1; this ratio has been shown by several studies in our laboratory [7,8,18,19] to be an optimum level of PP-*g*-MA for compatibilization of PP/organoclay mixtures.

Fig. 1 compares the WAXS scans for nanocomposites formed from PP/PP-*g*-MA/$M_2(HT)_2$ organoclay containing nominally 5 wt% montmorillonite, and the scans of the corresponding organoclays are also included for comparison. With the increased surfactant loading, the characteristic peak position for the pure organoclay largely shifts to lower angles, indicative of expanded galleries

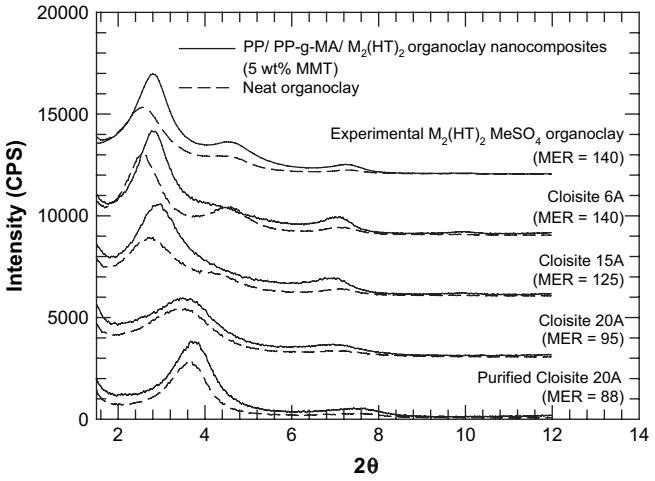

Fig. 1. WAXS scans for the $M_2(HT)_2$ pristine organoclays and PP/PP-*g*-MA/$M_2(HT)_2$ organoclay (ratio of PP-*g*-MA to organoclay = 1) nanocomposites containing ~5 wt% MMT. The curves are vertically offset for clarity.

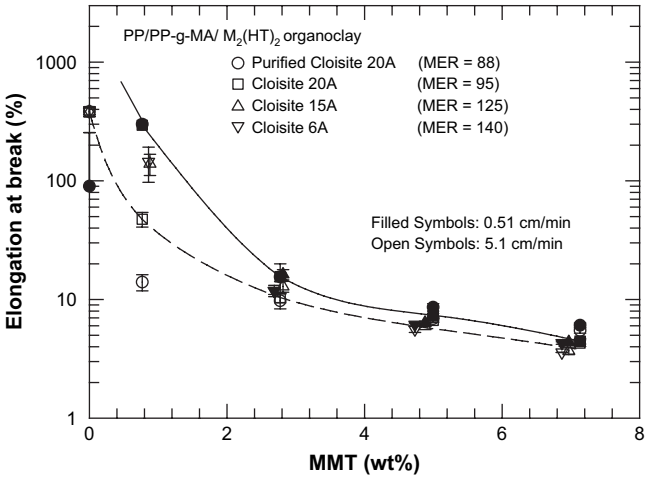

Fig. 3. Elongation at break measured at crosshead speeds of 0.51 cm/min and 5.1 cm/min for PP/PP-*g*-MA/$M_2(HT)_2$ organoclay (ratio of PP-*g*-MA to organoclay = 1) nanocomposites.

caused by this higher content of organic modifier. All the nanocomposites based on the various organoclays show similar, but not identical, X-ray peaks as the organoclay, indicating the presence of unexfoliated clay tactoids in these nanocomposites [8,16]. The relative peak positions follow a similar trend as the neat organoclays with various surfactant loadings. The peaks of the nanocomposites shift slightly to higher angles compared to that shown by the corresponding organoclay, which indicates a slight collapse of the clay gallery [16,20]; this phenomenon becomes more obvious as the surfactant loading of the organoclay increases. For $M_2(HT)_2^+MeSO_4^-$ organoclay with an MER of 140 mequiv/100 g of clay, similar shifting of the peak shown by the nanocomposite as compared to the organoclay can also be observed, although this organoclay has been shown to be significantly more thermally stable.

Nanocomposites based on PP/PP-*g*-MA/$M_2(HT)_2$ organoclay were prepared at several MMT loadings to obtain a more complete picture of the relative benefit of each organoclay with various organic loadings (MER) or purification levels. The addition of organoclay to the polymer matrix produces significant increases in the modulus in all cases (see Fig. 2); however, neither the purification nor the surfactant loading makes a significant difference in the observed tensile modulus of the nanocomposites formed from them. The nanocomposites based on organoclays (MER = 140 mequiv/100 g of clay) made from $M_2(HT)_2^+Cl^-$ and $M_2(HT)_2^+MeSO_4^-$ show very similar improvement in their tensile moduli, although there is a significant difference in the thermal stability of these two organoclays.

Fig. 3 compares the elongation at break for the PP nanocomposites. Two crosshead speeds, 0.51 cm/min and 5.1 cm/min, were used for the measurements. Generally, as the clay content is increased, ductility decreases dramatically for all the nanocomposites. The lower crosshead speed gave larger elongations at break as expected [21]; there are no obvious differences among the nanocomposites based on the various organoclays.

Fracture toughness as judged by the Izod impact strength is an important property to be considered for many applications. Polymer nanocomposites based on polyolefins have been reported to have different impact values for the gate end and far end of injection molded Izod bars [21]. Therefore, the impact strengths are averaged separately for the gate and far ends. Like the trends shown in elongation at break, there is a steady decrease in impact strength with increased clay content. The gate ends show slightly higher impact strength than the far ends, but these differences in this case are barely outside the error range (see Fig. 4).

Morgan and Harris reported similar work [1] using both unpurified and purified versions of organically modified fluorinated

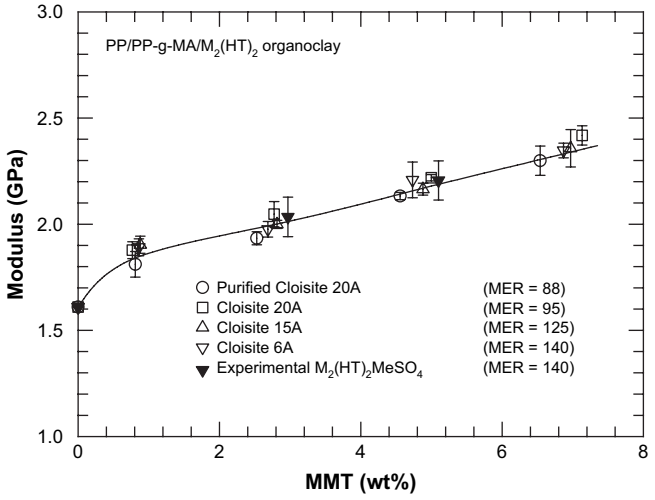

Fig. 2. Effect of MMT content on the tensile modulus of PP/PP-*g*-MA/$M_2(HT)_2$ organoclay (ratio of PP-*g*-MA to organoclay = 1) nanocomposites.

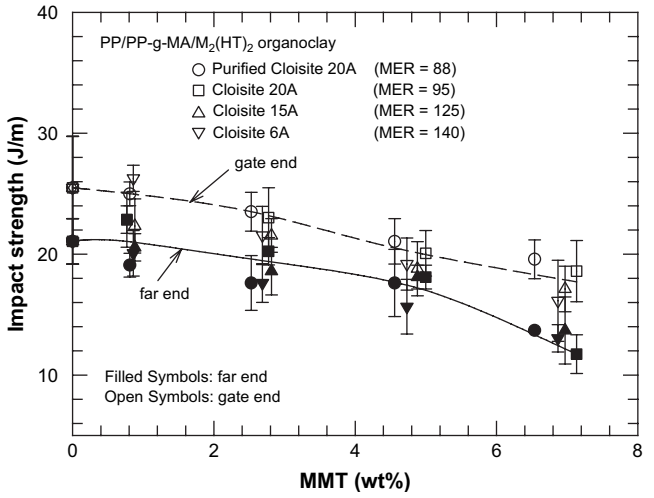

Fig. 4. Izod impact strength of gate-end and far-end samples of PP/PP-*g*-MA/$M_2(HT)_2$ organoclay (ratio of PP-*g*-MA to organoclay = 1) nanocomposites.

synthetic mica based clay, and they observed slight increases in flex modulus and slight decreases in impact strength by using ethanol Soxhlet extracted organoclays. However, the differences in properties of PP nanocomposites formed from as-received and purified (by methanol wash) organoclays in this study are negligible.

Appropriately prepared TEM images offer the most direct visualization of the dispersion of the clay particles in nanocomposites. Fig. 5 compares the morphology of polypropylene nanocomposites containing ~5 wt% MMT based on as-received $M_2(HT)_2$ organoclays with various surfactant loadings (MER values) and a purified version of Cloisite 20A. Morphologies consisting of combinations of individual platelets and platelet stacks can be observed in all the nanocomposites, indicating fair, but not complete exfoliation of the organoclays. Simple visual inspection of these images does not reveal any significant differences. A simple quantitative particle analysis of these images using similar methods described previously [12,16,22,23] was performed to explore more subtle differences. The number of clay particles in a given area of ~100 μm^2 was determined by analyzing 6–7 representative images like those in Fig. 5. From this count, a particle density, i.e., the number of clay particles per μm^2, was computed with the results shown in Table 2. The clay particle densities found for the nanocomposites based on as-received Cloisite 20A (MER = 95 mequiv/100 g of clay)

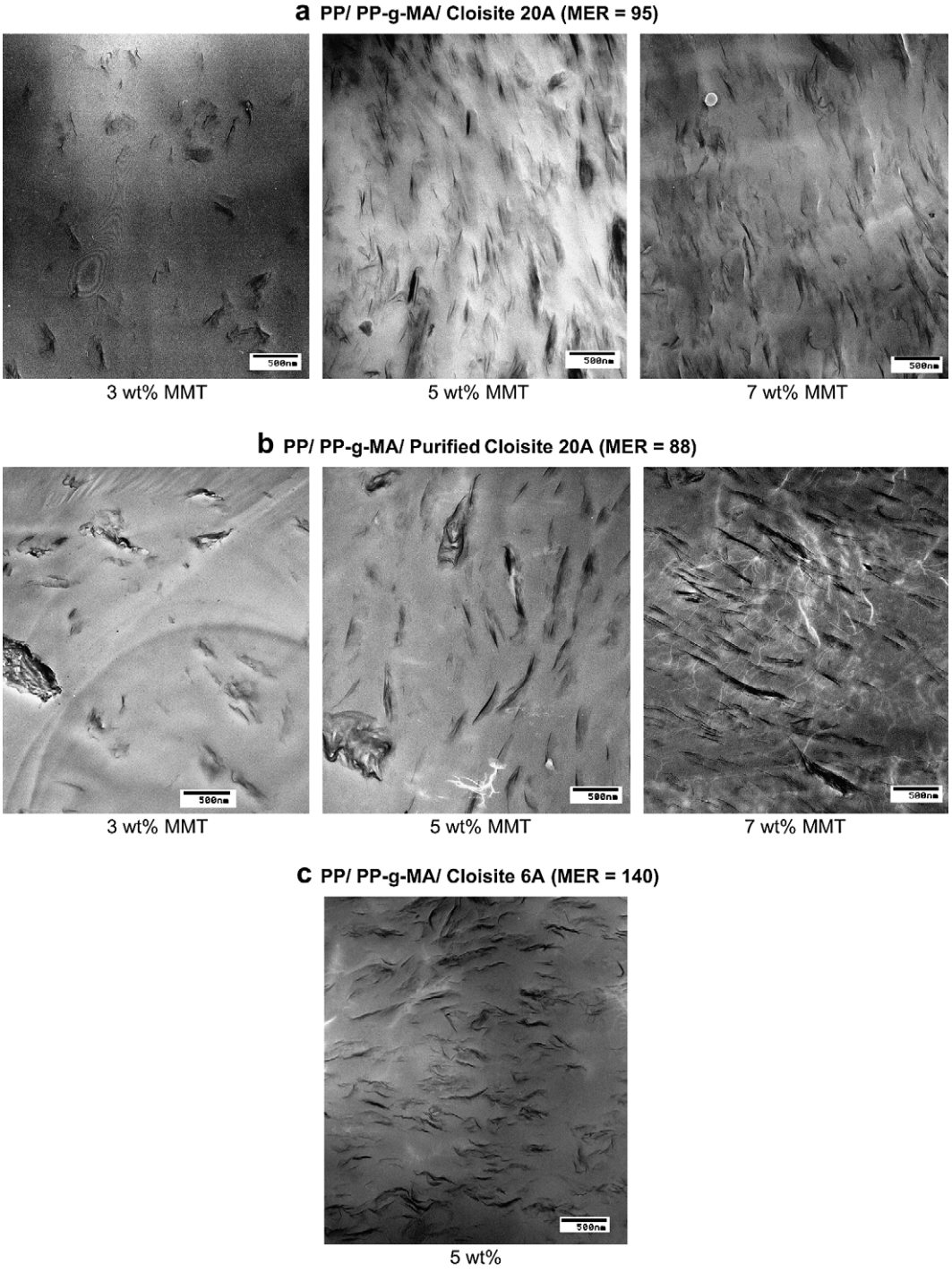

Fig. 5. TEM images of PP/PP-*g*-MA/$M_2(HT)_2$ organoclay (ratio of PP-*g*-MA to organoclay = 1) nanocomposites. The samples were taken from the core portion of an Izod bar and viewed parallel to the transverse direction.

Table 2
Particle density analysis of polypropylene nanocomposites

Sample (~5 wt% MMT)	Total area analyzed (μm^2)	Total number of particles	Particle density (particles/μm^2)
PP/PP-g-MA/Cloisite 20A	106	1330	12.5
PP/PP-g-MA/Cloisite 6A	105	1260	12.0
PP/PP-g-MA/purified Cloisite 20A	121	1000	8.3

and Cloisite 6A (MER = 140 mequiv/100 g of clay) were about the same. However, for the nanocomposite formed from purified Cloisite 20A (MER = 88 mequiv/100 g of clay) the clay particle density was found to be somewhat less. Higher clay particle densities mean that the organoclay has been dispersed more effectively with a small number, on average, of aluminosilicate platelets per particle. Based on this analysis, it appears that polypropylene nanocomposites formed from as-received Cloisite 20A and Cloisite 6A give slightly better exfoliation of the organoclay than the ones formed form purified Cloisite 20A. One possible explanation for this phenomenon is that the removal of surfactant molecules from around the platelets edges in the purified organoclay reduces the wetting of the clay by the non-polar polypropylene, and, thus, somewhat poorer dispersion [1]. In the end, however, this difference in degree of dispersion does not have a significant effect on mechanical properties as seen in Figs. 2–4.

3.2. PA-6 nanocomposites

Two single-tail organoclays, $M_3(HT)_1$ (MER = 95 mequiv/100 g of clay) and $M_3(C16)_1$ (MER = 100 mequiv/100 g of clay), were used to explore the effect of organoclay purification on the properties of the nanocomposites formed. The purification of the organoclays removes most of the excess surfactant; as a result, both organoclays are left with a lower MER around 85 mequiv/100 g of clay.

The WAXS scans of nylon 6 nanocomposites prepared from purified and as-received $M_3(HT)_1$ and $M_3(C16)_1$ organoclays are shown in Figs. 6 and 7. After purification, both organoclays have slightly smaller basal spacings due to the removal of excess surfactant from the clay galleries. In contrast to the results for nanocomposites based on polypropylene, nylon 6 nanocomposites do not show any X-ray peaks characteristic of the corresponding neat organoclays, indicative of the possibility of well-exfoliated structures [12,17,24] regardless of the purification of the organoclays.

Tensile moduli of nanocomposites formed from nylon 6 and $M_3(HT)_1$ organoclays are compared in Figs. 8 and 9. The moduli data

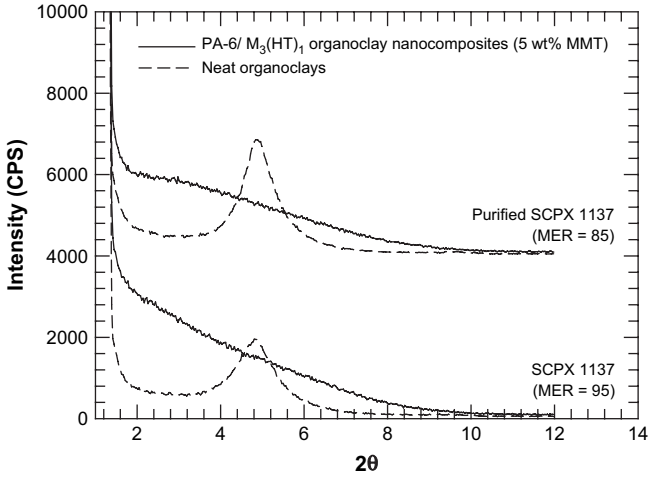

Fig. 6. WAXS scans for the $M_3(HT)_1$ pristine organoclays and PA-6/$M_3(HT)_1$ organoclay nanocomposites containing ~5 wt% MMT. The curves are vertically offset for clarity.

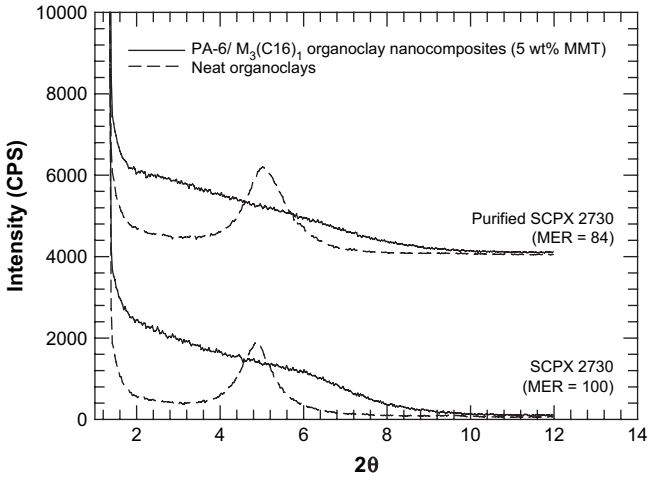

Fig. 7. WAXS scans for the $M_3(C16)_1$ pristine organoclays and PA-6/$M_3(C16)_1$ organoclay nanocomposites containing ~5 wt% MMT. The curves are vertically offset for clarity.

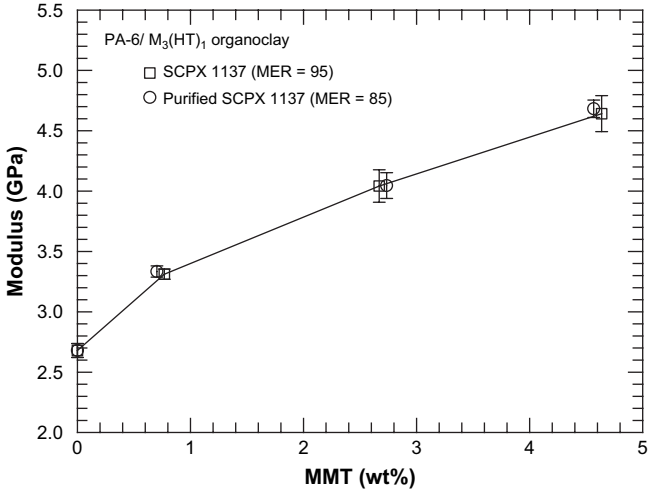

Fig. 8. Effect of MMT content on the tensile modulus of PA-6/$M_3(HT)_1$ organoclay nanocomposites.

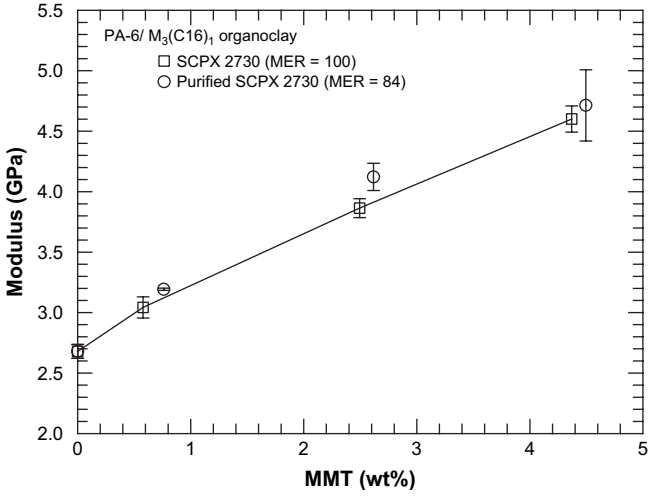

Fig. 9. Effect of MMT content on the tensile modulus of PA-6/$M_3(C16)_1$ organoclay nanocomposites.

for nanocomposites formed from both $M_3(HT)_1$ and $M_3(C16)_1$ organoclays do not show any meaningful differences between the as-received and purified versions.

Figs. 10 and 11 compare the elongation at break of these nanocomposites at various MMT contents for two rates of extension. As expected, samples show higher ductility when strained at lower speeds, and their ductility decreases as the MMT content is increased. The elongation at break data have relatively large standard deviations; however, it appears that the nanocomposites formed from the purified organoclays, denoted by solid or open circles, exhibit somewhat lower ductility. Currently there is no plausible explanation for this reduction in elongation at break for the nanocomposites formed from purified organoclays.

Figs. 12 and 13 show the notched Izod impact strength data for the various nylon 6 nanocomposites at room temperature. Values from the far and gate ends of injection molded samples were averaged since the difference between the two is relatively small [11,17]. The impact strength data have relatively large standard deviations. Both nanocomposite systems show a decrease in impact strength as the clay content is increased; while the mean values from the Izod test appear slightly lower for some of the compositions containing purified organoclay relative to the as-received version, these differences are not judged to be statistically meaningful in view of the standard deviations in the data.

The effects of organoclay purification on the exfoliation level in PA-6/$M_3(HT)_1$ organoclay and PA-6/$M_3(C16)_1$ organoclay nanocomposites are corroborated by the pictorial evidence provided by the TEM images in Figs. 14 and 15. Very well-exfoliated morphologies can be observed in all the PA-6 nanocomposites. Similar quantitative particle density analyses as described earlier were conducted to explore the subtle differences in these PA-6 nanocomposites. The results are shown in Table 3. Some differences in the clay particle densities were found when comparing the

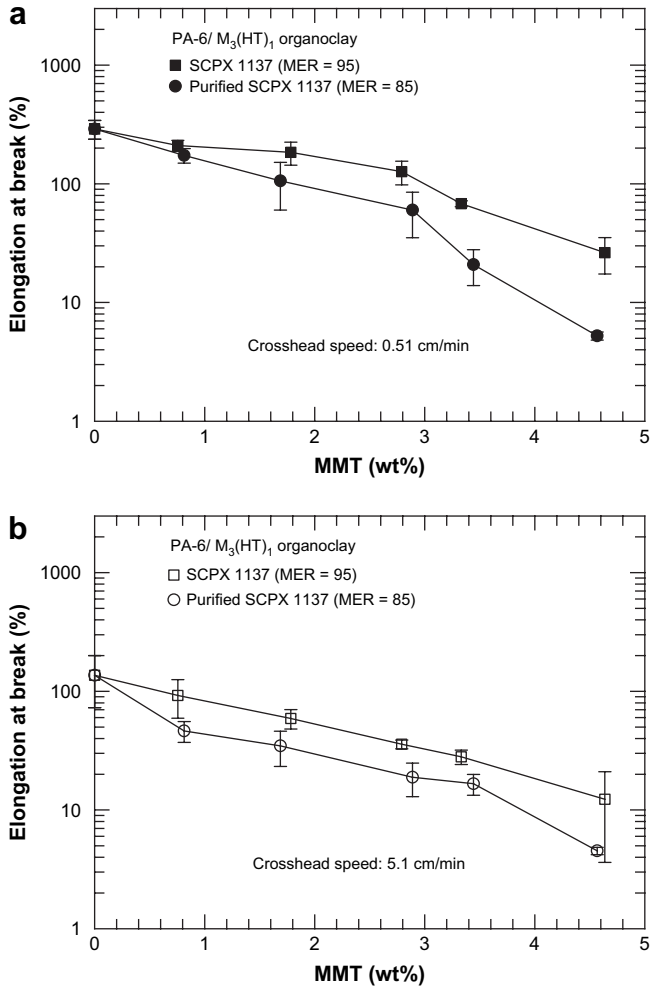

Fig. 10. Elongation at break for PA-6/$M_3(HT)_1$ organoclay nanocomposites measured at crosshead speeds of (a) 0.51 cm/min and (b) 5.1 cm/min.

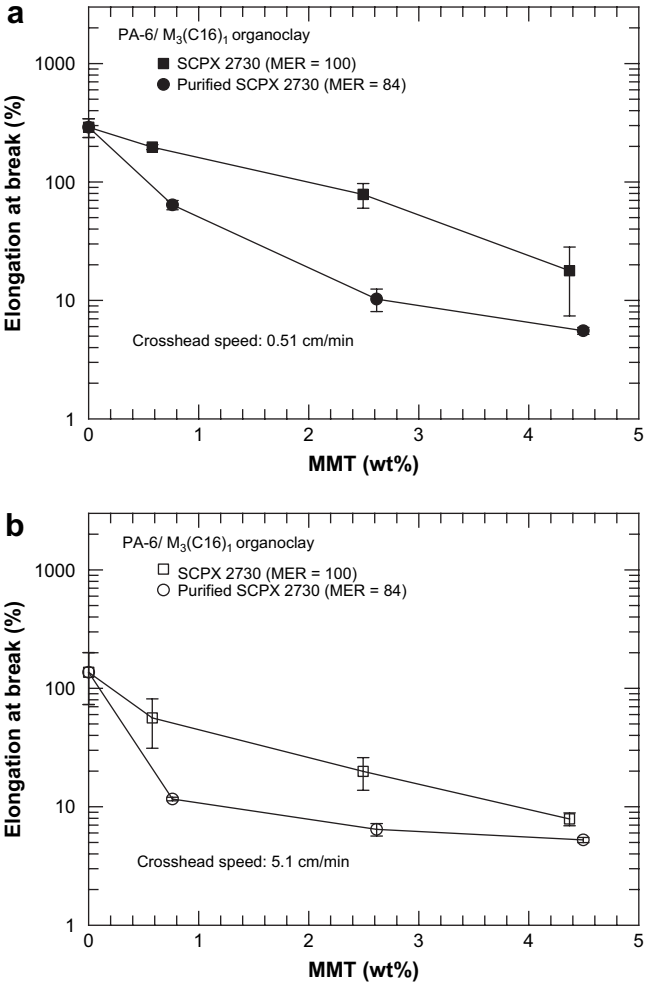

Fig. 11. Elongation at break for PA-6/$M_3(C16)_1$ organoclay nanocomposites measured at crosshead speeds of (a) 0.51 cm/min and (b) 5.1 cm/min.

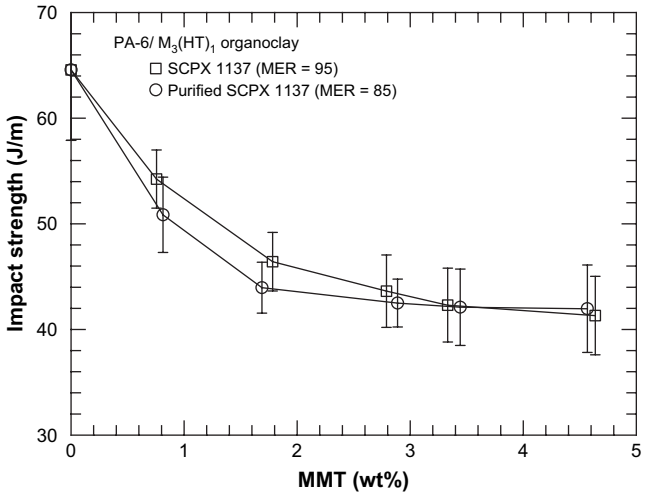

Fig. 12. Izod impact strength of PA-6/$M_3(HT)_1$ organoclay nanocomposites.

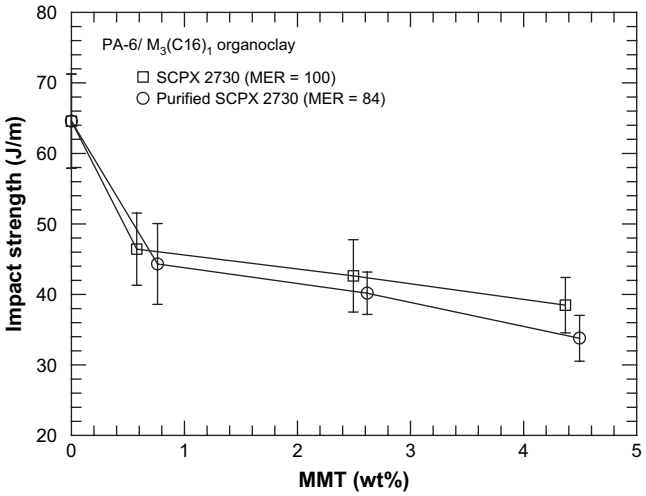

Fig. 13. Izod impact strength of PA-6/$M_3(C16)_1$ organoclay nanocomposites.

nanocomposites formed from the $M_3(HT)_1$ and $M_3(C16)_1$ organoclays; the ones formed from the $M_3(C16)_1$ organoclays, either as-received or purified versions, have larger particle densities compared to the ones formed from the $M_3(HT)_1$ organoclays. However, in contrast to polypropylene nanocomposites, the clay particle densities for these PA-6 nanocomposites based on purified and as-received versions of the same organoclay were about the same. Since the polar polyamide interacts better with the hydrophilic silicate platelets than the organic surfactant, removal of the excess surfactant does not affect the morphologies of the PA-6 nanocomposites although the differences in the thermal stability of the purified and as-received organoclays are significant.

4. Conclusions

Two series of organoclays, two-tail organoclays, i.e., $M_2(HT)_2$ organoclays, with various levels of excess surfactant, and as-received or purified single-tail organoclays, $M_3(HT)_1$ and $M_3(C16)_1$ organoclays, were selected to form polypropylene and nylon 6 nanocomposites, respectively, and to explore the effect of organoclay degradation or the presence of excess surfactant on morphology and properties of nanocomposites as evaluated by TEM, WAXS and mechanical tests (tensile and Izod).

As reported in Part 1 of this series, the purification level and surfactant loadings of organoclay significantly affect their thermal stability; however, broadly speaking, the results from the various characterization techniques are consistent with each other suggesting that these differences in thermal stability do not appear to have much effect on the morphology and properties of the nanocomposites formed from them. For polypropylene nanocomposites formed from the $M_2(HT)_2$ organoclays,

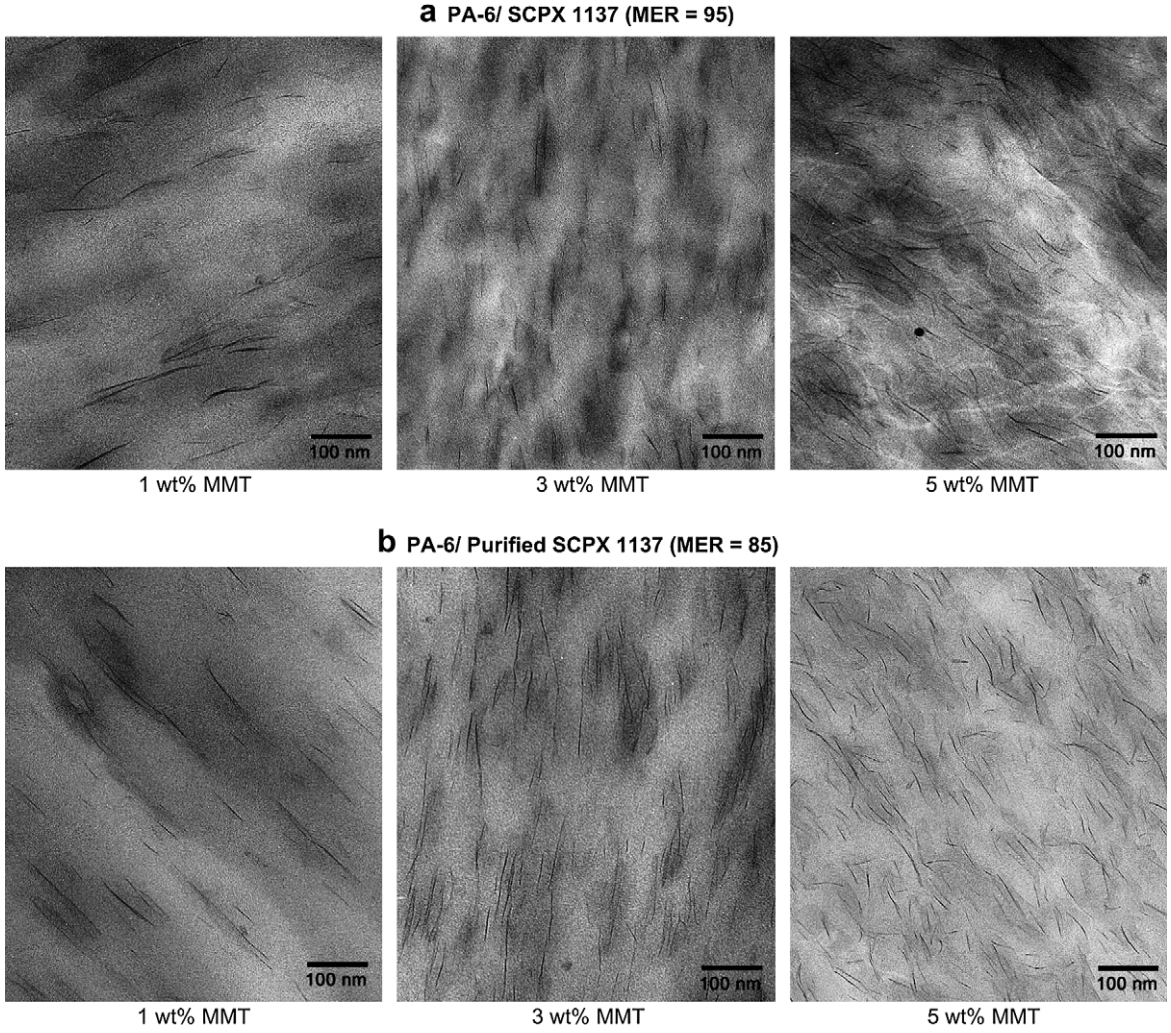

Fig. 14. TEM images of PA-6/$M_3(HT)_1$ organoclay nanocomposites. The samples were taken from the core portion of an Izod bar and viewed parallel to the transverse direction.

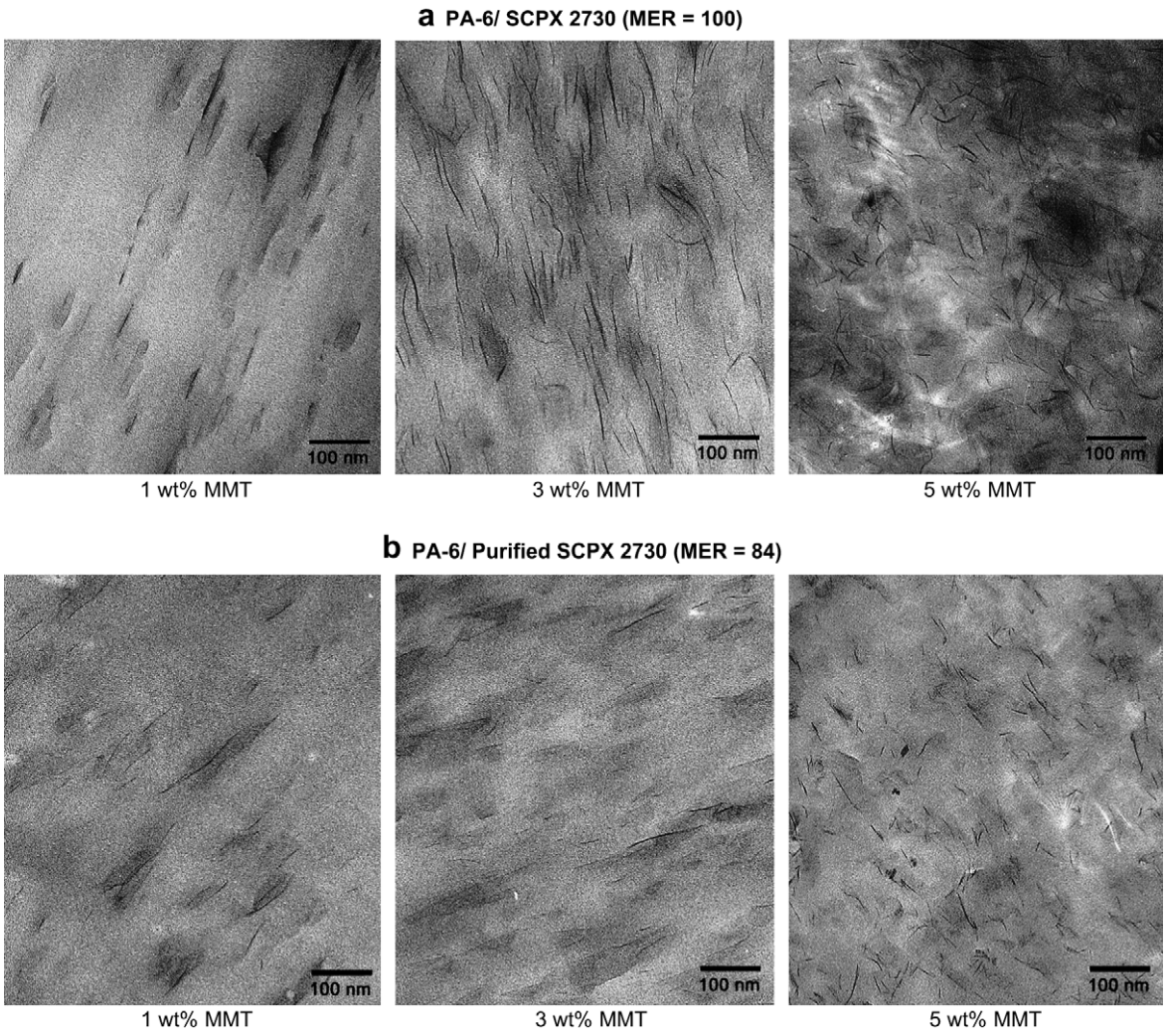

Fig. 15. TEM images of PA-6/$M_3(C16)_1$ organoclay nanocomposites. The samples were taken from the core portion of an Izod bar and viewed parallel to the transverse direction.

Table 3
Particle density analysis of PA-6 nanocomposites

Sample (~5 wt% MMT)	Total area analyzed (μm^2)	Total number of particles	Particle density (particles/μm^2)
PA-6/$M_3(HT)_1$ organoclay	3.65	1130	310
PA-6/purified $M_3(HT)_1$ organoclay	3.35	1060	320
PA-6/$M_3(C16)_1$ organoclay	3.65	1330	360
PA-6/purified $M_3(C16)_1$ organoclay	3.66	1410	380

purification of Cloisite 20A organoclay appears to have some adverse effects on the organoclay dispersion, but it does not have a significant effect on mechanical properties. For PA-6 nanocomposites, purification of the as-received organoclays does not significantly alter the morphology or the mechanical properties of these nanocomposites with the exception of some reduction in elongation at break, for which there is no plausible explanation.

It could be argued that the degradation of the surfactant would be detrimental to dispersion or exfoliation of the organoclay. However, it should be remembered that both degradation and exfoliation in the extruder are rate processes; it is possible that, in some cases, the exfoliation/dispersion process is completed on a time scale before degradation has progressed to a detrimental level.

References

[1] Morgan AB, Harris JD. Polymer 2003;44(8):2313–20.
[2] Osman MA, Mittal V, Suter UW. Macromolecular Chemistry and Physics 2007; 208(1):68–75.
[3] Davis RD, Gilman JW, Sutto TE, Callahan JH, Trulove PC, De Long HC. Clays and Clay Minerals 2004;52(2):171–9.
[4] Cui L, Khramov DM, Bielawski CW, Hunter DL, Yoon PJ, Paul DR. Part 1 of this series. Polymer 2008;49(17):3751–61.
[5] Fornes TD, Yoon PJ, Hunter DL, Keskkula H, Paul DR. Polymer 2002;43(22): 5915–33.
[6] Fornes TD, Hunter DL, Paul DR. Macromolecules 2004;37(5):1793–8.
[7] Kim DH, Fasulo PD, Rodgers WR, Paul DR. Annual Technical Conference – Society of Plastics Engineers 2006;64:592–6.
[8] Lee H-S, Fasulo PD, Rodgers WR, Paul DR. Polymer 2005;46(25):11673–89.
[9] Shah RK, Hunter DL, Paul DR. Polymer 2005;46(8):2646–62.
[10] Hotta S, Paul DR. Polymer 2004;45(22):7639–54.
[11] Yoon PJ, Hunter DL, Paul DR. Polymer 2003;44(18):5323–39.
[12] Chavarria F, Paul DR. Polymer 2004;45(25):8501–15.
[13] Huang JJ, Paul DR. Polymer 2006;47(10):3505–19.
[14] Huang JJ, Keskkula H, Paul DR. Polymer 2006;47(2):624–38.
[15] Yoon PJ, Fornes TD, Paul DR. Polymer 2002;43(25):6727–41.
[16] Kim DH, Fasulo PD, Rodgers WR, Paul DR. Polymer 2007;48(20):5960–78.
[17] Fornes TD, Yoon PJ, Keskkula H, Paul DR. Polymer 2001;42(25):09929–40.
[18] Lee H-S, Fasulo PD, Rodgers WR, Paul DR. Polymer 2006;47(10):3528–39.
[19] Cui L, Paul DR. Polymer 2007;48(6):1632–40.
[20] Shah RK, Paul DR. Polymer 2006;47(11):4075–84.
[21] Shah RK, Cui L, Williams KL, Bauman B, Paul DR. Journal of Applied Polymer Science 2006;102(3):2980–9.
[22] Cui L, Ma X, Paul DR. Polymer 2007;48(21):6325–39.
[23] Dennis HR, Hunter DL, Chang D, Kim S, White JL, Cho JW, et al. Polymer 2001; 42(23):9513–22.
[24] Fornes TD, Paul DR. Macromolecules 2004;37(20):7698–709.